Synthesis and Mass Spectrometry Studies of an Amphiphilic Polyether-Based Rotaxane That Lacks an Enthalpic Driving Force for Threading

Kathleen M. Wollyung,[†] Kaitian Xu,[‡] Michael Cochran,[‡] Andrea M. Kasko,[‡] Wayne L. Mattice,[‡] Chrys Wesdemiotis,*[,†] and Coleen Pugh*[,‡]

Department of Chemistry, The University of Akron, Akron, Ohio 44325-3601, and Department of Polymer Science, Maurice Morton Institute of Polymer Science, The University of Akron, Akron, Ohio 44325-3909

Received November 12, 2004; Revised Manuscript Received January 7, 2005

ABSTRACT: A pure amphiphilic macrocrown ether (MC-12) was obtained by removing linear oligomers and larger macrocycles at the macrocyclization step, before proceeding with an established synthetic procedure. This pure MC-12 was used to synthesize a rotaxane composed of one MC-12 ring threaded with one end-capped poly(tetrahydrofuran) (PTHF) oligomer by equilibrating half an equivalent of the thread with an organized solution of MC-12 and end-capping the threads with excess 2-*p*-[tris(*p*-*tert*-butylphenyl)methyl]phenoxymethyl-4,4-dimethylazlactone. The rotaxane was positively identified by matrix-assisted laser desorption/ionization time-of-flight (MALDI-ToF) mass spectrometry (MS), although the spectra showed a low abundance of the rotaxane ions and high abundances of unthreaded MC-12 and end-capped thread ions in the product isolated from the threading experiment. Analysis by GPC was inconclusive because both the rotaxane and a one-to-one complex elute at the same retention volume. MALDI-ToF and electrospray ionization quadrupole ion trap (ESI-QIT) MS analyses of the rotaxane sample and mixtures of MC-12 and end-capped thread, including studies using varying laser intensities, comparisons of linear and reflectron analysis modes of the ToF MS, and analysis of the rotaxane by the post-source decay method demonstrated that the rotaxane does not fragment during the MALDI-ToF MS analysis, although the rotaxane ionizes less efficiently than either of its two components. HPLC using silica columns and an eluant of THF with 0.3 wt % Aliquat 336 confirmed that a "further-purified" sample of the rotaxane mixture was composed of 66 wt % end-capped thread, 23 wt % MC-12, and 11 wt % rotaxane, in qualitative agreement with the corresponding MALDI-ToF mass spectrum.

Introduction

Rotaxanes are physical complexes of a cyclic molecule threaded with a linear molecule that is end-capped at both ends with bulky groups to prevent dethreading;[1,2] polyrotaxanes are composed of multiple cycles threaded with an end-capped linear polymer.[2,3] The original motivation for synthesizing polyrotaxanes was to study the predicted unusual solution and solid-state properties of molecules that are simply a physical entrapment of noninteracting cyclic and linear molecules. This architectural effect can only be studied using *homo*polyrotaxanes, which are composed of chemically identical cycles and threads, since their properties must be compared to those of both the linear and cyclic components. However, only *hetero*polyrotaxanes with extremely strong interactions between chemically different cycles and threads are readily accessible due to the resulting large enthalpic driving force for threading. The synthesis of noninteracting homopolyrotaxanes has been largely abandoned due to the low efficiencies of statistical threading in entropically controlled systems.

We previously proposed that homorotaxanes and homopolyrotaxanes that lack an enthalpic driving force for threading, such as those based on macrocrown ethers threaded with poly(ethylene oxide) (PEO) or poly(ethylene glycol) (PEG), may potentially be synthesized in higher yield by an amphiphilic approach.[4] This approach is based on the ability of amphiphilic macrocycles to form organized micellar solutions in solvents that selectively solvate an attached tail.[5] If an added thread is also not soluble in the selective solvent, it will be forced into the interior of the micelle (Scheme 1), where the high concentration and alignment of the macrocycles should promote threading. Although we have not yet mimicked this three-component system using simulations, we have recently used Monte Carlo simulations to investigate both the effect of solvent quality[6] and the alignment[7] of the macrocycles on the extent of threading 42-crown-14 with $CH_3(OCH_2CH_2)_{13}OCH_3$; we previously found that 42-crown-14 is approximately the optimum ring size for maximum spontaneous threading by PEO with inconsequential multiple threading.[8] Compared to the melt (1.73 threading events = 4.33% of the rings threaded),[8] the number of threading events decreases with solvent dilution since there are fewer rings present, and the percentage of rings threaded are lower in the good and Θ solvents than in the melt and poor solvent.[6] This indicates that threading is favored by aggregation in a poor solvent. In addition, planar alignment can double the extent of threading (to 9% of the rings threaded) compared to the purely statistical threading in the melt, if the distance between cycles in two consecutive layers is confined to a distance approximately equal to the size of the rings.[7]

One of the most conclusive methods for positively identifying a threaded structure is characterization by a technique such as mass spectrometry (MS) of a high molecular weight compound whose molecular weight

[†] Department of Chemistry.
[‡] Department of Polymer Science.
* To whom correspondence should be addressed.

10.1021/ma0476689 CCC: $30.25
Published on Web 03/05/2005

Scheme 1. Amphiphilic Approach for Synthesizing Polyrotaxanes that Lack an Enthalpic Driving Force for Threading

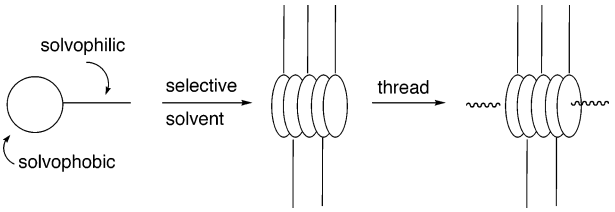

and chemical composition correspond to the sum of a combination of the cyclic and linear components. Our previous threading experiment attempted to characterize the product(s) of threading 3,4-(42-crown-14)benzyl dodecyl ether (MC-12)[9] with PEG3350-bisamine (3350 Da) in an organized solution by matrix-assisted laser desorption/ionization Fourier transform (MALDI−FT) MS, but the results were inconclusive;[4] i.e., a high molecular weight compound was apparently present, but its molecular weight was too high to accurately identify. In addition, since the MALDI−FT MS characterization did not become available to us until the end of our initial studies, we found that the MC-12 used was composed not only of cyclic unimer but also of approximately 17% of its cyclic dimer, which NMR spectroscopy cannot differentiate. This paper therefore first reports the synthesis and purification of MC-12, in which the purity of the product from each reaction step was confirmed by matrix-assisted laser desorption/ionization time-of-flight (MALDI-ToF) MS before proceeding to the next step.

To optimize the MS conditions for identifying (poly)rotaxanes based on polyethers, this paper also reports the synthesis and MALDI-ToF MS, electrospray ionization quadrupole ion trap (ESI-QIT) MS, and MS/MS characterization of a low molecular weight rotaxane of MC-12 threaded with bis(3-aminopropyl)-terminated poly(tetrahydrofuran)-350 (PTHF, 350 Da), with future work advancing to polyrotaxanes of longer chains threaded with more rings, using our amphiphilic approach for threading. Although the resulting rotaxane is not formally a *homo*rotaxane, both components are aliphatic polyethers. In addition, the use of a PTHF thread instead of PEO was very useful for differentiating the molecular weight distributions of the ring (EO repeat units) and the thread (THF repeat units) in the mass spectra of the rotaxane and thereby positively identifying the rotaxane. Mixtures of MC-12 and end-capped thread were analyzed using varying laser intensities in both linear and reflectron MALDI-ToF modes, and the rotaxane was analyzed by the post-source decay MS/MS method to determine whether the ionization efficiencies of the rotaxane varied significantly from those of its components. Analyses were performed to determine whether peaks in the MALDI-ToF MS spectrum were from unreacted components not removed during purification of the rotaxane or whether they were from fragmentation of the rotaxane during the MALDI-ToF MS analysis, with the results confirmed by compositional analysis using high-performance liquid chromatography (HPLC).

Experimental Section

Materials. Acetic acid (Fisher, glacial), Aliquat 336 (Acros), bis(3-aminopropyl)-terminated PTHF350 (Aldrich, $M_n \sim 350$ Da), and 3,4-dihydroxybenzaldehyde (Acros, 97%) were used as received. The bismesylate of poly(ethylene glycol)-600 and 2-*p*-[tris(*p*-*tert*-butylphenyl)methyl]phenoxymethyl-4,4-dimethylazlactone were synthesized as described previously.[4] Dimethylformamide (DMF) was distilled from and stored over molecular sieves. Dry CH_2Cl_2 was obtained by washing with 10% HNO_3 in H_2SO_4, neutralizing with dilute aqueous $NaHCO_3$ and water, storing over $CaCl_2$, and then distilling from CaH_2 under N_2. Hexanes were washed with 5% HNO_3 in H_2SO_4, neutralized with dilute aqueous $NaHCO_3$ and water, stored over $CaCl_2$, and then distilled from purple sodium benzophenone ketyl under N_2. Toluene was dried by distillation from purple sodium benzophenone ketyl under N_2. Column and flash chromatography were performed using silica gel (65−250 mesh (63−200 μm), 60 Å pore) or basic activated alumina (150 mesh (63−200 μm), 58 Å pore).

2,5-Dihydroxybenzoic acid (DHB) (Aldrich, 99%), indoleacrylic acid (IAA) (Aldrich, 98%), and dithranol (1,8,9-anthracenetriol, Fluka, 99%) were used as received as matrices for MALDI-ToF MS analyses, with long-term storage in a desiccator, as were the sodium, silver, potassium, and lithium trifluoroacetate salts (NaTFA, AgTFA, KTFA, each 98%, and LiTFA, 95%, Aldrich). Tetrahydrofuran (THF) (Aldrich, HPLC 99.9%, inhibitor free) and methanol (Aldrich, 99.93% ACS Grade) solvents were used as received for MALDI-ToF MS sample preparation. MALDI-ToF MS calibrants included poly(methyl methacrylate) standard ($M_n = 2000$ Da) (Fluka, pdi $= M_w/M_n \sim 1.10$) and polystyrene standards ($M_n \sim 1800$ and 5700 Da, pdi < 1.15) (supplied by Prof. Roderic Quirk, The University of Akron).

Techniques. All reactions were performed under a N_2 atmosphere using a Schlenk line unless noted otherwise. ^{1}H (300 MHz) NMR spectra (δ, ppm) were recorded in $CDCl_3$ using a Mercury 300 spectrometer. The resonances were measured relative to residual solvent resonances and referenced to tetramethylsilane. Gel permeation chromatography (GPC) was performed at 35 °C using THF as eluant (1.0 mL/min), a set of 50, 100, 500, 10^4, and linear ($50-10^4$) Å and guard Styragel 5 μm columns, a Waters 410 differential refractometer (RI), and/or a Waters 486 tunable UV/vis detector set at 254 nm. HPLC was performed at 35 °C using THF containing 0.3% (w/w) Aliquat 336 as eluant (1.0 mL/min), a semipreparative silica gel column plus an analytical silica gel column (both 125 Å pores, 10 μm particle size), and a Waters 486 tunable UV/vis detector set at 254 nm.

MALDI-ToF MS experiments were carried out using a Bruker Daltonics Reflex III mass spectrometer equipped with a 337 nm nitrogen laser and a pulsed ion extraction source. Data were collected in both linear and reflectron detection modes using the two-stage grid-less reflector for improved resolution. The ion source and reflector lens potentials were held at 20 and 22.5 keV, respectively. The polymer samples were dissolved in THF at 10 mg/mL in polyethylene centrifuge tubes and used on the same day. The salts (NaTFA, AgTFA, KTFA, or LiTFA) were dissolved in THF at 10 mg/mL in polyethylene centrifuge tubes. DHB, IAA, and dithranol matrices were each dissolved in THF at 20 mg/mL in polyethylene centrifuge tubes. The salt and matrix solutions were used on the same day or stored in a freezer and allowed to return to room temperature before use; they were never stored longer than 2 weeks. Aliquots of the matrix, polymer, and salt solutions were mixed in a 5:2:1 ratio unless noted otherwise, and 0.5 μL of the final mixture was applied to the stainless steal sample target for analysis. Tandem mass spectra (MS^2) of the rotaxane oligomers were acquired in the MALDI-ToF instrument using post-source decay; fragmentation after the ions leave the source region is caused by metastable decomposition of the ions or by collisions with residual gas molecules. The reflectron analyzer voltage was increased in steps over a series of collected spectra. Each reflectron voltage fully focused a different fragment mass range (or energy range), and appropriate mass ranges were pasted together to create the composite spectrum.

ESI-QIT mass spectra were acquired with a Bruker Daltonics Esquire-LC mass spectrometer. Polymer samples were dissolved in THF to form 0.1 mM solutions, which were diluted

with THF/methanol (1:9 v/v) to 10^{-5} M, and a solution of NaTFA in THF was added to the polymer solution for a final salt concentration of 10^{-5} M. The final analyte solutions were infused directly into the spray chamber using a Cole-Parmer syringe pump (300 μL/h). A potential of −4 kV was applied to the entrance of the sampling capillary, which is orthogonal to the grounded spraying needle. Nitrogen served as the nebulizer gas (15 psi) and drying gas (5 L/min at 300 °C). These conditions yielded singly charged $[M + Na]^+$ adduct ions of the oligomers. MS^2 of MC-12 and end-capped thread oligomers were acquired using the ESI-QIT mass spectrometer. The desired $[M + Na]^+$ precursor ions (complete isotopic cluster) were isolated in the trap and then induced to fragment via collisionally activated dissociation (CAD). The excitation time in the trap was 40 ms, and the rf amplitude was adjusted within 1.25−1.8 V to decrease the intensity of the isolated precursor ions by at least 50%.

The resolution of the reflectron-mode ToF and QIT analyzers was sufficient for obtaining resolved isotopic patterns. Therefore, the mass-to-charge ratios (*m/z*) quoted are monoisotopic; i.e., they refer to the oligomer peak containing the lowest-mass isotopes (^{12}C, ^{1}H, ^{16}O, ^{14}N, ^{23}Na). Since singly charged ions were formed upon MALDI and ESI under the analysis conditions used, the *m/z* value of an ion and the mass of this ion in Da have identical numerical values.

Synthesis of 3,4-(42-Crown-14)benzyl Dodecyl Ether (MC-12). MC-12 was synthesized as described previously,[4] except that we established a procedure for removing linear oligomers and larger cyclic oligomers from 3,4-(42-crown-14)-benzaldehyde (MC-CHO), before proceeding to subsequent steps. We will therefore reproduce only the synthesis of MC-CHO and report its purification here. A solution of 3,4-dihydroxybenzaldehyde (2.85 g, 20.6 mmol) and PEG-600 bismesylate (15.1 g, 20.2 mmol) in DMF (200 mL) was added dropwise over 16 h to a slurry of finely ground K_2CO_3 (8.51 g, 61.6 mmol) in DMF (100 mL) at 70 °C. The temperature was then raised to 125 °C, and the mixture was stirred for 72 h. After the reaction mixture was cooled to room temperature, it was filtered to remove the potassium salts, and DMF was distilled off under reduced pressure. The residue was dried in vacuo at 60 °C for 6 h to yield 14.2 g of a brown oil. MALDI-ToF MS of this crude product demonstrated that it contained linear and larger cyclic oligomers in addition to the desired cyclic unimer. The crude product was passed through a column of silica gel (415 g, 6 cm diameter, 38 cm long) using methanol/$CHCl_3$ (5:4 v/v, 1000 mL) as the eluant to obtain 12.9 g (93.2%) of an oil, which contained primarily the cyclic oligomers, especially cyclic unimer, contaminated with a small amount of linear oligomers according to MALDI-ToF MS. (Although most of the linear oligomers remained on the column, they will elute with additional solvent, especially if the polarity of the eluant is increased by increasing the amount of methanol.) The remaining linear oligomers were removed from this material by a second column chromatography purification using the same conditions to obtain 10.6 g of cyclic oligomers as a light brown oil. Pure MC-CHO (2.69 g of cyclic unimer, 19.4%) was isolated as a light yellow oil by Soxhlet extraction of the cyclic mixture supported on silica (∼12 g) using hexanes for 96 h. (Additional MC-CHO can be obtained by extracting out the mixture of cyclic oligomers from the silica support using THF or methanol and repeating the Soxhlet extraction of the oil supported on a minimum amount of silica using hexanes.) The remaining steps in the synthesis of MC-12 proceeded as described previously.[4]

Synthesis of Poly(tetrahydrofuran)-350 Thread End-Capped with 2-*p*-[Tris(*p*-*tert*-butylphenyl)methyl]phenoxymethyl-4,4-dimethylazlactone. A solution of bis(3-aminopropyl)-terminated PTHF350 (0.10 g, 0.57 mmol NH_2 end groups) and 2-*p*-[tris(*p*-*tert*-butylphenyl)methyl]phenoxymethyl-4,4-dimethylazlactone (0.80 g, 1.3 mmol) in CH_2Cl_2 (30 mL) was stirred at room temperature for 140 h, and then 1 M glacial acetic acid (150 mL, 150 mmol) was added. After stirring at room temperature for 24 h, the solvents were removed by rotary evaporation, and the residue was dried in vacuo to yield 0.62 g of a slightly yellow solid. The powder was dissolved and passed through a short column of basic activated alumina using methanol/CH_2Cl_2 (1:30 v/v) as both the solvent and eluant. After removing the solvent by rotary evaporation, 0.38 g (79%) of the end-capped thread was obtained as a white powder. ^1H NMR: 1.30 (s, C*H*$_3$ of *t*-Bu, 54 H), 1.60 (br s, C*H*$_3$ and C*H*$_2$CH$_2$O, 24 H), 1.77 (p, C*H*$_2$CH$_2$N, 4 H), 3.40 (m, C*H*$_2$O and N*H*, 16 H), 3.52 (t, C*H*$_2$N, 4 H), 4.41 (s, OC*H*$_2$CO, 4 H), 6.82 (d, 4 aromatic H *ortho* to OCH$_2$), 7.09 (d, 12 aromatic H *meta* to *t*-Bu), 7.14 (d, 4 aromatic H *ortho* to OCH$_2$), 7.25 (dd, 12 aromatic H *ortho* to *t*-Bu).

Threading Experiment of MC-12 with Poly(tetrahydrofuran)-350. A solution (42.4 wt % MC-12/15.2 wt % H_2O/42.4 wt % hexanes, $[H_2O]:[EO] = 1.3$) of MC-12 (0.50 g, 0.57 mmol) and water (180 μL, 9.9 mmol) in hexanes (0.50 g) was stirred at room temperature for 1 h. The bis(3-aminopropyl)-terminated PTHF350 thread (0.10 g, 0.29 mmol) was added all at once, and the mixture was stirred at room temperature for 28 h. 2-*p*-[Tris(*p*-*tert*-butylphenyl)methyl]phenoxymethyl-4,4-dimethylazlactone (0.55 g, 0.87 mmol) was then added, and the mixture stopped stirring. After standing at room temperature for 96 h, CH_2Cl_2 (10 mL) was added, and the mixture was stirred for another 24 h at room temperature. The mixture was then diluted with additional CH_2Cl_2 (30 mL), 1 M acetic acid (150 mL, 0.15 mol) was added to hydrolyze the excess end-capping agent, and the solution was stirred at room temperature for 24 h. The solvents were removed in vacuo, and the resulting yellowish solid residue was dispersed in CH_2Cl_2 (40 mL). The hydrolyzed excess end-capping agent (69 mg, 35%) was removed as a white powder by filtration. Solvent was removed from the filtrate by rotary evaporation, and the resulting slightly yellowish solid (1.1 g) was dissolved in methanol/CH_2Cl_2 (1:30 v/v) and passed through a short column of basic activated alumina using methanol/CH_2Cl_2 (1:30 v/v) as the eluant to remove the remaining hydrolyzed excess end-capping agent. After removing the solvent by rotary evaporation, 0.84 g (118%) of the "crude" rotaxane product was obtained as a slightly yellow solidlike material. The crude product was then purified by column chromatography using silica gel as the stationary phase and methanol/$CHCl_3$/hexanes (1:15:3 v/v/v) as the eluant to obtain 0.58 g (82%) of the "original" rotaxane sample as a white solid from the second chromatography fraction; the first eluted fraction (10 mg) was composed only of the end-capped PTHF thread, and a third fraction (0.22 g) obtained by eluting the column with methanol/$CHCl_3$ (1:5 v/v) was an oil composed primarily of MC-12. ^1H NMR spectroscopy confirmed that the "crude" product and "original" sample contained resonances of both MC-12 and the end-capped thread. (^1H NMR spectroscopy cannot differentiate between threaded and unthreaded structures in this system.) MALDI-ToF MS indicated that the "original" sample was composed primarily of unthreaded MC-12, with a lesser amount of free end-capped PTHF thread and a small amount of rotaxane. A "further purified" sample (0.31 g, 44%) was obtained as a white powder by precipitating the "original" sample from THF (3 mL) into hexanes (75 mL); 0.26 g of a waxy material was recovered from the filtrate. MALDI-ToF MS of the "further purified" sample indicated that much of the unthreaded MC-12 had been removed, consistent with ^1H NMR spectroscopy.

Results and Discussion

Synthesis, Purification, and MALDI-ToF MS Characterization of MC-12. Although we previously synthesized MC-12 in relatively high yield by the route outlined in Scheme 2, it produced not only the distribution of ring sizes corresponding to "monodisperse" PEG600 (600 Da) but also ∼17% of the cyclic dimer after purification. We have therefore repeated this synthesis and confirmed that the product of each step was pure by MALDI-ToF MS before proceeding to the next step. The most important step in the synthesis is the macrocyclization of PEG600-bismesylate with 3,4-dihy-

Scheme 2. Synthesis of 3,4-(42-Crown-14)benzyl Dodecyl Ether (MC-12) Starting from the Bismesylate of Poly(ethylene glycol)-600 (600 Da); DMF = Dimethylformamide

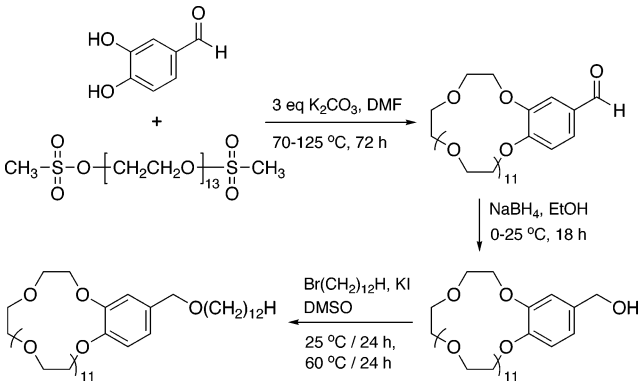

droxybenzaldehyde under pseudo-high-dilution conditions in the presence of multiple potassium template ions. Figure 1 presents the MALDI-ToF mass spectra of the resulting 3,4-(42-crown-14)benzaldehyde (MC-CHO) before and after purification. Since K_2CO_3 was used in the synthesis of MC-CHO, we initially analyzed these samples with KTFA as the cationization salt. However, there were still abundant Na^+ adduct ions in these spectra due to the ubiquitous sodium from glassware in reaction vessels and solvent bottles. The spectra using Na^+ spiking, such as that of pure MC-CHO in Figure 1c, are therefore more simplified than with K^+.

The spectrum of the crude macrocyclization product, which is typically a brown oil or waxy material, is presented in Figure 1a. The distribution of masses centered at *m/z* 715 are due to MC−CHO; those centered at *m/z* 1430 are due to the cyclic dimer, and those centered at *m/z* 2145 are due to the cyclic trimer. The additional distributions that are more obvious at the baseline of the spectrum are due to PEG and linear oligomers of $HO[(CH_2CH_2O)_n-C_7H_4O_2]_xH$. The cyclic oligomers (Figure 1b) were isolated from the linear oligomers by column chromatography using silica gel as the stationary phase and collecting the first fraction eluted with methanol/$CHCl_3$ (5:4). (The linear oligomers can be isolated with additional eluant, especially if the polarity of the eluant is increased by increasing the proportion of methanol.) The unimeric MC-CHO was finally isolated from the cyclic mixture by Soxhlet extraction of the oils supported on a minimum amount of silica using hexanes; since the solubility of polymers decreases as their molecular weight increases, the cyclic unimer is extracted first. However, much of the cyclic unimer is also retained on the silica support. Although the yield increases as the synthesis and purification are scaled up since less silica can be used, this is the step in the purification that could be improved.

Nevertheless, the spectrum shown in Figure 1c demonstrates that the linear and larger cyclic oligomers have been removed and that the macrocycle is pure. In particular, there are a series of peaks at the expected intervals of 44.0 Da, corresponding to the distribution of C_2H_4O (EO) units of the macrocycle. The measured *m/z* values of the $[MC\text{-}CHO + Na]^+$ ions correlate well with the values calculated for MC-CHO oligomers having the $C_7H_4O_2$ "terminal" group. For example, the peak at *m/z* 671.3 matches within experimental error (<0.5 *m/z* units) the *m/z* value (671.13) calculated for monoisotopic $[(EO)_{12}-C_7H_4O_2 + Na]^+$. The macrocycles

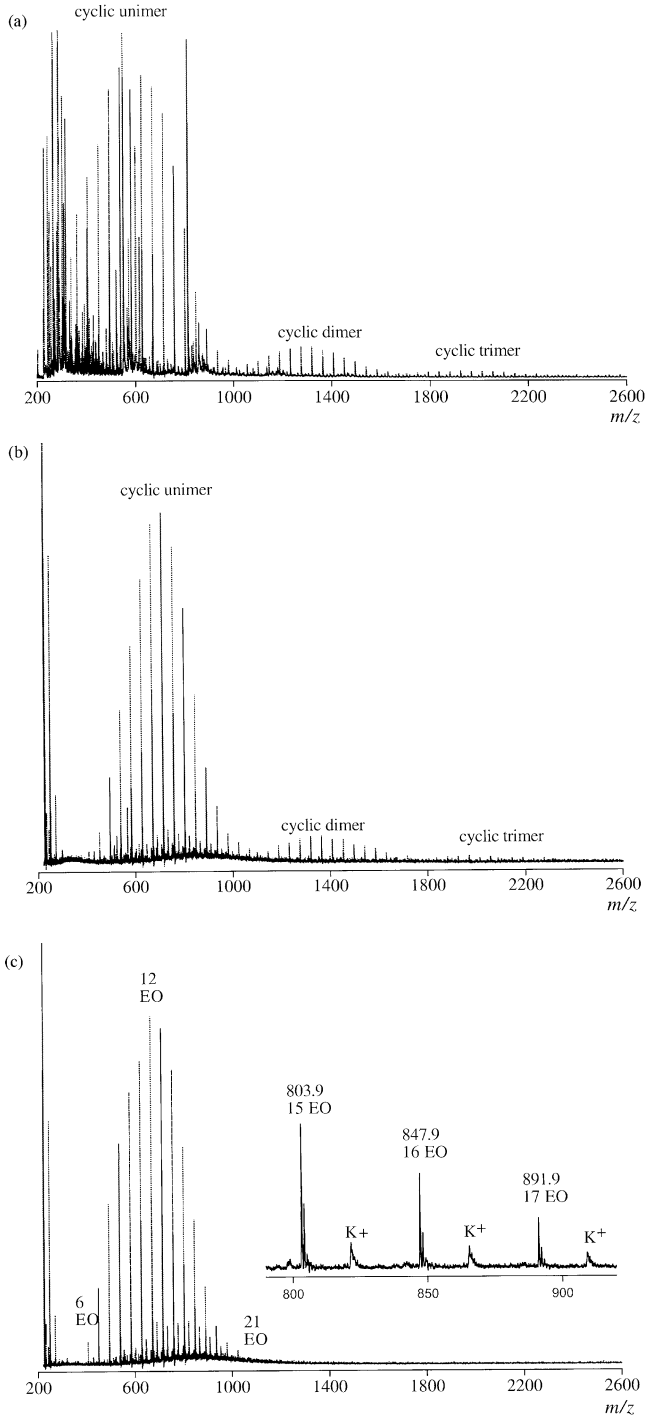

Figure 1. Matrix-assisted laser desorption/ionization time-of-flight mass spectra (dithranol matrix, sodium trifluoroacetate salt, reflectron mode) of 3,4-(42-crown-14)benzaldehyde (MC-CHO) synthesized from the bismesylate of poly(ethylene glycol)-600 (600 Da): (a) crude product; (b) cyclic components isolated as the first fraction from column chromatography of the crude product using silica as the stationary phase and methanol/$CHCl_3$ (5:4 v/v) as the eluant; (c) pure macrocycle obtained by Soxhlet extraction of the cyclic mixture using hexanes.

observed in the spectrum contain 6−21 EO units. Although the nominal molecular weight of PEG-600 corresponds to 13 repeat units, the ring present in the highest concentration in this spectrum has $n = 12$ EO units and 39 atoms in the ring but varies from 9 to 12 EO units in repetitions of the synthesis and purification of MC-CHO.

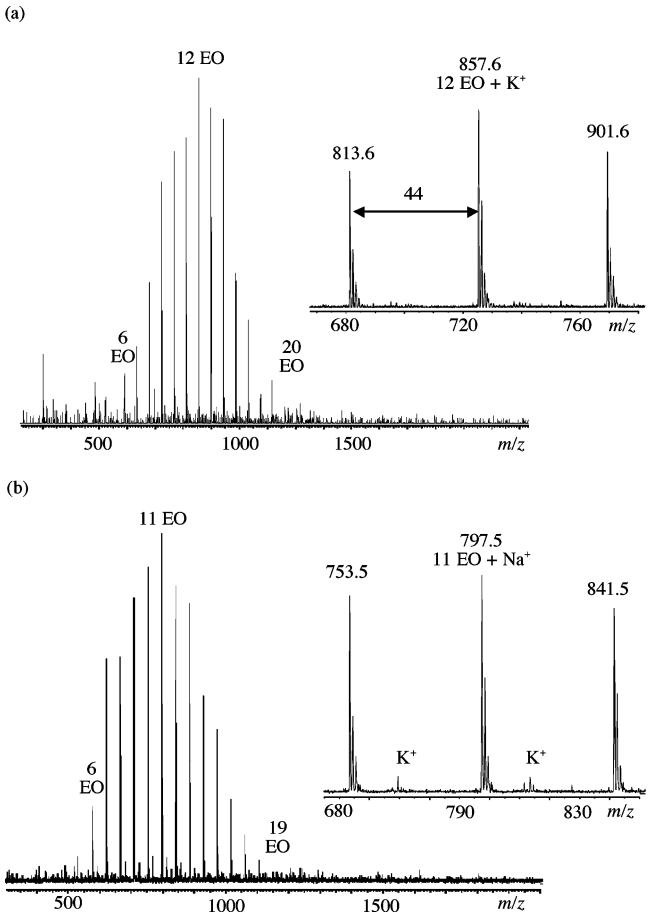

Figure 2. Matrix-assisted laser desorption/ionization time-of-flight mass spectra of MC-12 with (a) K^+ ions (potassium trifluoroacetate salt) and (b) Na^+ ionization (sodium trifluoroacetate salt); dithranol matrix, reflectron mode.

The remaining steps in the synthesis of MC-12 proceeded as outlined in Scheme 2, with the aldehyde group of MC-CHO reduced using sodium borohydride and the resulting benzyl alcohol etherified with *n*-bromododecane. The MALDI-ToF mass spectra of MC-12 using both NaTFA and KTFA are presented in Figure 2 and demonstrate that it is free of both linear and higher order cyclic oligomers. The MALDI-ToF mass spectra again show a series of peaks at the expected intervals of 44.0 Da, consistent with the EO repeat units. The measured *m/z* values of the $[MC\text{-}12 + K]^+$ and $[MC\text{-}12 + Na]^+$ ions (Figure 2, a and b, respectively) correlate well with the values calculated for MC-12 oligomers having the expected $C_{19}H_{30}O_2$ "terminal" group with a monoisotopic mass of 290.2 Da. For example, the peak at *m/z* 857.6 (Figure 2a) matches within experimental error (<0.5 *m/z* units) the *m/z* value calculated for monoisotopic $[(EO)_{12}-C_{19}H_{30}O_2 + K]^+$ (857.5), and the peak at *m/z* 797.5 (Figure 2b) matches the *m/z* value calculated for monoisotopic $[(EO)_{11}-C_{19}H_{30}O_2 + Na]^+$ (797.4). The $[MC\text{-}12 + K]^+$ distribution extends from 6 to 20 EO units, with the 11- or 12-mer being the most abundant oligomer (multiple analyses), while the $[MC\text{-}12 + Na]^+$ distribution contains 6−19 EO units, with the most abundant oligomer being the 11-mer. The oligomer distributions vary slightly because the larger K^+ ion can more easily coordinate with larger oligomers than the smaller Na^+ ion.[10] The number of EO units in the most abundant macrocycle varies from $n = 9-12$ in repeated syntheses and purifications of MC-12.

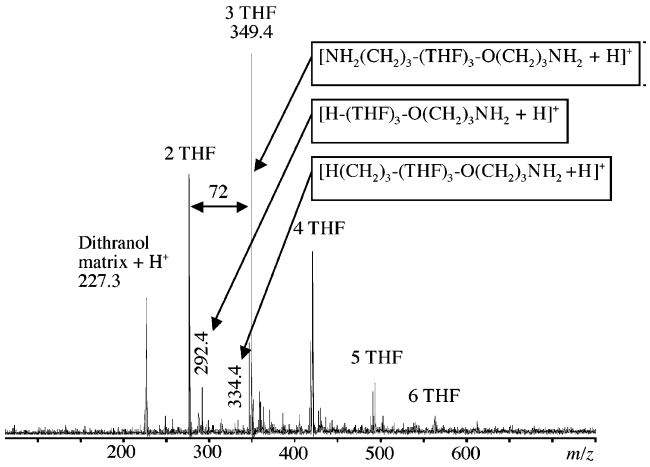

Figure 3. Matrix-assisted laser desorption/ionization time-of-flight mass spectrum of bis(3-aminopropyl)-terminated poly(tetrahydrofuran)-350 (~350 Da); dithranol as matrix, reflectron mode.

Synthesis and MALDI-ToF MS Characterization of the End-Capped PTHF Thread. Before synthesizing the end-capped thread, we first analyzed the bis(3-aminopropyl)PTHF350 commercial reactant by MALDI-ToF MS. As shown in Figure 3, no metal cationizing salt was needed since this amine-containing low molecular weight sample generates $[M + H]^+$ ions. The spectrum shows that the *m/z* values of the main distribution are $72.1m + 133.1$ Da, which correspond to the distribution of $C_4H_8O_2$ (THF) repeat units of the oligomer plus a mass of 132.1 for the $-(CH_2)_3NH_2$ and $-O(CH_2)_3NH_2$ end groups of the thread. For example, the most intense peak at *m/z* 349.4 matches the (monoisotopic) mass calculated for the ion of the nominal structure of bis(3-aminopropyl)PTHF350 $[NH_2(CH_2)_3-(THF)_3-O(CH_2)_3NH_2 + H]^+$ (349.4 Da). The $m = 2-6$ oligomers are also observed.

As outlined in Scheme 3, the commercial bisamine is undoubtedly synthesized by reacting the PTHF-diol with acrylonitrile by a Michael-like addition, followed by reduction of the cyano groups to amines. Although the nitrile intermediates are not detectable in the spectrum, a minor distribution corresponding to functionalization of only one of the diol end groups is detected at 57 Da below the main distribution. For example, the peak at *m/z* 292.4 agrees with $[H-(OCH_2CH_2CH_2CH_2)_3-O(CH_2)_3NH_2 + H]^+$ (monoisotopic mass of 292.4 Da). A second minor distribution at 15 Da below the main distribution is attributable to threads with a propyl substituent without the terminal amine group at one chain end; the peak at *m/z* 334.4 represents $[H(CH_2)_3-(THF)_3-O(CH_2)_3NH_2 + H]^+$, whose theoretical mass is 334.4 Da. Both minor impurities may decrease the yield slightly of end-capped thread and rotaxane; i.e., the alkyl end group is completely unreactive toward the azlactone, whereas ring-opening of the azlactone by an alcohol requires long reaction times or acid or base catalysis,[11] in contrast to primary amines, which react at room temperature in the absence of a catalyst,[11] even in dilute aqueous solutions.[12] We have not identified the other minor peaks present in Figure 3.

The end-capped thread was synthesized by reacting bis(3-aminopropyl)PTHF350 with excess 2-*p*-[tris(*p*-*tert*-butylphenyl)methyl]phenoxymethyl-4,4-dimethylazlactone in the absence of the macrocycle (Scheme 3), both to optimize the purification procedure for removing

Scheme 3. Retrosynthetic Analysis of Bis(3-aminopropyl)-Terminated Poly(tetrahydrofuran) and Its Reaction with 2-*p*-[Tris(*p*-*tert*-butylphenyl)methyl]phenoxymethyl-4,4-dimethylazlactone to Produce the End-Capped Thread

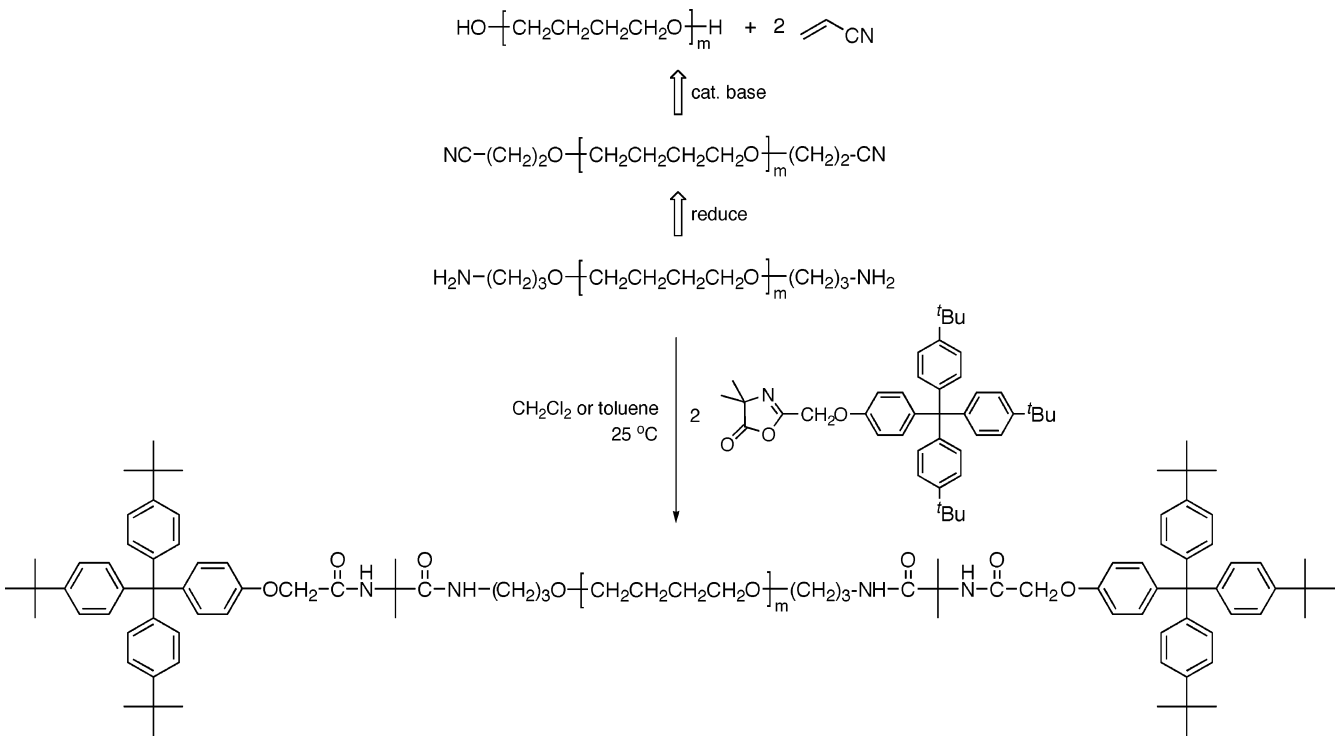

unreacted azlactone from the threading experiments and to obtain end-capped thread for characterization. The bisamine reacts with the azlactone by a ring-opening addition reaction to generate an amide bond. Since the end-capping reaction in the rotaxane synthesis involves a large excess of the end-capping agent, we established conditions for hydrolyzing the excess azlactone using 0.1 N aqueous acetic acid and removed it as the ring-opened *N*-(2-isobutyric acid)-*p*-[tris(*p*-*tert*-butylphenyl)methyl]phenoxyacetamide; although the excess end-capping agent can also be hydrolyzed with 0.1 N aqueous HCl, these conditions cannot be used for the threading experiments since they also hydrolyze the hydrocarbon segment from MC-12. The resulting isobutyric acid can then be removed by passing the mixture through a short column of basic activated alumina or recycled back into the azlactone synthesis by isolating it as an insoluble material in a dispersion of the product mixture in CH_2Cl_2; any remaining traces of hydrolyzed end-capping agent can then be removed by passing the end-capped thread through a plug of basic activated alumina.

The MALDI-ToF mass spectrum of the end-capped thread (ECT) presented in Figure 4 shows an abundant series of peaks with a repeat unit of 72.1 Da, corresponding to the distribution of $C_4H_8O_2$ (THF) units in the thread. The measured *m/z* values correspond to $[ECT + Na]^+$ ions having the expected end groups with a combined mass of 1390.9 Da. For example, the peak at *m/z* 1629.9 matches within experimental error (<0.5 *m/z* units) the *m/z* value calculated for monoisotopic $[C_{46}H_{59}N_2O_3-(THF)_3-C_{46}H_{59}N_2O_4 + Na]^+$ (1630.1). The number of THF units in the end-capped thread (*m*) varies from two to six, as with bis(3-aminopropyl)-PTHF350. A second, minor, distribution (cf. peaks at *m/z* 1663.8 and 1591.8) exists in the spectrum which, based on the *m/z* values of its peaks, is related to the main distribution by a mass decrease of 38 Da. This series may originate from monofunctional $[H-(OCH_2CH_2CH_2CH_2)_mC_{46}H_{59}N_2O_4 + Na]^+$ ions with a longer sequence of THF repeat units. For example, the peak

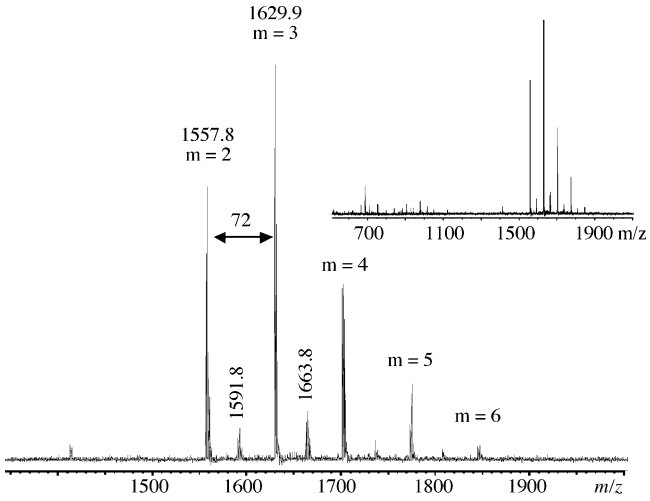

Figure 4. Matrix-assisted laser desorption/ionization time-of-flight mass spectrum of poly(tetrahydrofuran)-350 (~350 Da) thread end-capped with 2-*p*-[tris(*p*-*tert*-butylphenyl)methyl]phenoxymethyl-4,4-dimethylazlactone; dithranol as matrix, sodium trifluoroacetate salt, reflectron mode.

at *m/z* 1591.8 represents the corresponding 12-mer (calculated *m/z* at 1592.1). The inset in Figure 4 shows the full mass range of the spectrum. No peaks are observed for either the original bis(aminopropyl)-terminated thread or a thread with only one end-cap, i.e., $[NH_2(CH_2)_3-(OCH_2CH_2CH_2CH_2)_3-C_{46}H_{59}N_2O_4 + Na]^+$ (*m/z* 1000.7 not observed), although there is a trace amount of monofunctional $H-(OCH_2CH_2CH_2CH_2)_3-C_{46}H_{59}N_2O_4$ in the *m/z* 900−1000 region. Therefore, the MALDI-ToF MS data confirm that this reaction proceeds efficiently at both $-NH_2$ ends of the thread.

Scheme 4. Threading Experiment of an Organized Solution of MC-12 Ring with Bis(3-aminopropyl)-Terminated Poly(tetrahydrofuran)-350, Followed by End-Capping with 2-*p*-[Tris(*p*-*tert*-butylphenyl)-methyl]phenoxymethyl-4,4-dimethylazlactone

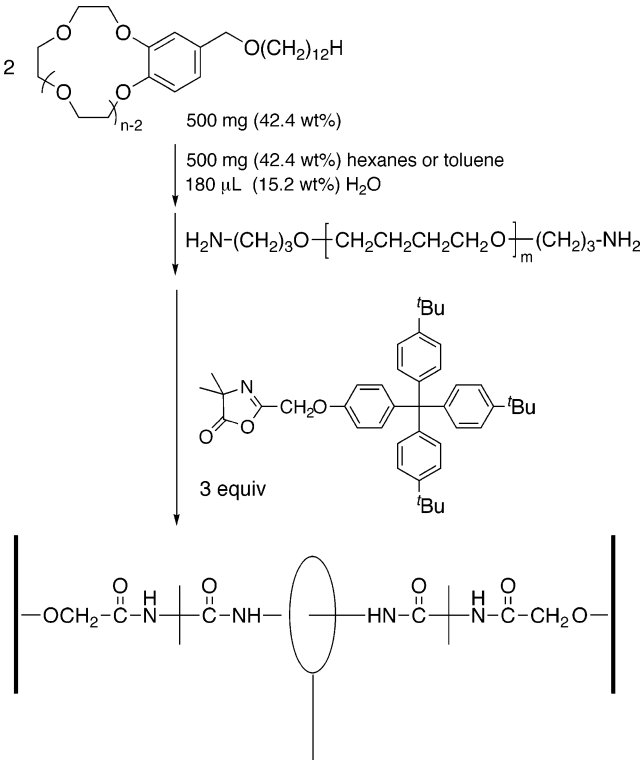

Synthesis and Characterization of the Rotaxane of MC-12 Threaded with PTHF. MC-12 forms a lyotropic lamellar (L_α) mesophase in hydrocarbon solvents if small amounts of water are added.[4,5,13] Scheme 4 outlines the threading procedure, in which 2 equiv of MC-12 was equilibrated with bis(3-aminopropyl)-terminated PTHF350 in hexanes in the presence of 17 equiv H_2O ($[H_2O]:[EO] = 1.3$), before adding 1.5 equiv of the end-capping agent (relative to the amine end groups of the thread); the results are similar using toluene as the selective organic solvent. Excess unreacted end-capping agent was removed by hydrolyzing it with 1 M aqueous acetic acid and isolating the resulting isobutyric acid as the insoluble material in a dispersion of the product mixture in CH_2Cl_2, followed by passing the product mixture through basic activated alumina to remove any remaining traces of hydrolyzed end-capping agent. We then attempted to separate the rotaxane from unthreaded MC-12 and unreacted end-capped thread using column chromatography. The resulting material was a semisolid, in contrast to MC-12 and the bisamine PTHF thread, which are oils.

As discussed above, identification of a species that has a higher molecular weight than either the end-capped thread or cyclic components would be the most convincing evidence for the formation of threaded structures. Unfortunately, GPC using polystyrene columns is inconclusive. For example, a mixture of MC-12 and end-capped thread elute both as isolated species in THF (44.2 and 42.5 mL, respectively) and apparently as a complex that elutes at lower elution volume (40.7 mL), corresponding to higher molecular weight, to generate a chromatogram similar to that of the solid material isolated from the threading experiment (Figure 5); i.e., the solid material isolated from the threading experiment contains at least some unthreaded MC-12 and end-capped thread as well as (poly)rotaxane and/or an unthreaded complex of the two. This demonstrates how difficult it can be to separate a rotaxane from its cyclic and linear components when they are based on identical or similar chemical structures. It also indicates that the composition of the (poly)rotaxane and the cycle/thread complex are similar, assuming that the isolated solid material contains some rotaxane or polyrotaxane. The polystyrene-equivalent molecular weight (2500 Da) of the material that elutes at 40.7 mL in Figure 5 corresponds to one MC-12 cycle threaded or complexed with one end-capped thread.

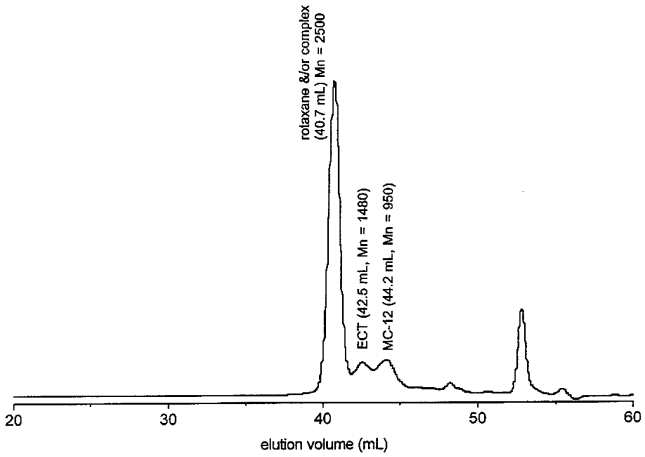

Figure 5. Gel permeation chromatogram of the "original sample" of the rotaxane of MC-12 threaded with bis(3-aminopropyl)-terminated poly(tetrahydrofuran)-350; 5 μm polystyrene (PSt) columns, THF as eluant; PSt equivalent molecular weights.

We therefore investigated conditions for characterizing the molecular weights of the components of the (poly)rotaxane mixture by MS and for quantifying its composition by HPLC. A typical MALDI ToF mass spectrum of the mixture, measured with NaTFA as the cationization salt and dithranol as the matrix, is displayed in Figure 6a. The spectrum consists of three sets of peaks. The lowest mass series of peaks is from unthreaded MC-12 with C_2H_4O repeat units (44.0 Da) and the expected end group with a mass of 290.2 Da. The second series of peaks is from end-capped thread with C_4H_8O (72.1 Da) repeat units and the expected combined end groups of 1390.9 Da. The third set of peaks of low intensity must be due to rotaxane ions, with a mass corresponding to that of one MC-12 ring threaded with one end-capped PTHF molecule.

Because of the low signal intensity of the rotaxane, we reanalyzed this sample using different instrument parameters, starting with variation of the matrix and cationization salt, to enhance the ion abundance and signal-to-noise ratio of the rotaxane ions. Although both IAA and 2,4-DHB are useful in synthetic polymer analysis,[14] the rotaxane ion formation was not enhanced in these matrices with NaTFA (spectra not shown). We also analyzed the rotaxane using AgTFA, which often complexes with double bonds or phenyl groups,[15] in each of the three matrices to determine whether the *tert*-butyltrityl end groups would promote formation of $[M + Ag]^+$ ions. Similarly, we tested LiTFA because lithium cations bind to heteroatoms more strongly than sodium cations, and complexation with lithium depends less on the availability of multiple coordination sites due to its smaller size.[16] The resulting spectra (not shown)

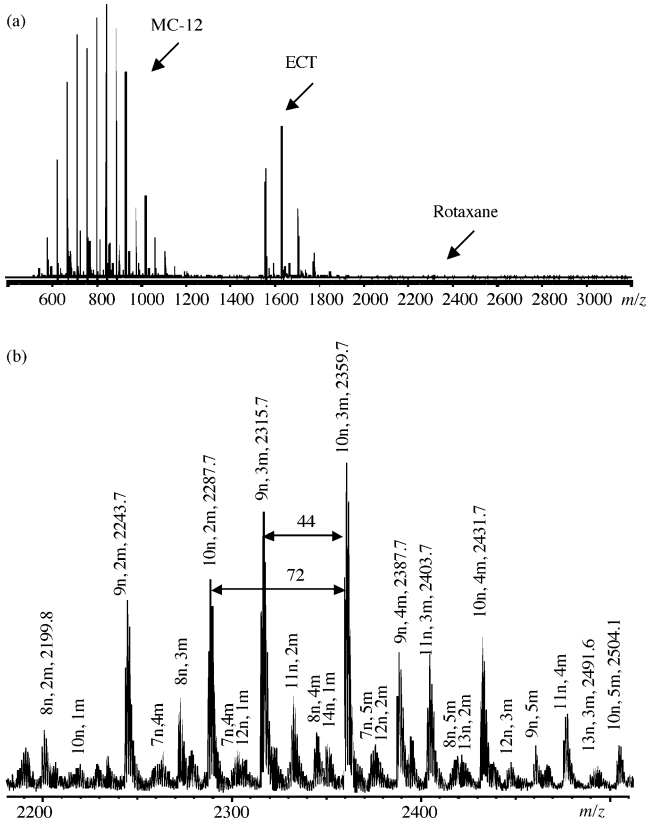

Figure 6. Matrix-assisted laser desorption/ionization time-of-flight mass spectra (dithranol matrix, sodium trifluoroacetate salt, reflectron mode) of the "original" rotaxane sample of MC-12 threaded with bis(3-aminopropyl)-terminated poly(tetrahydrofuran)-350: (a) full mass range (30% of maximum laser intensity); (b) expanded view of the rotaxane region collected with increased deflection of low mass ions (m/z < 2000) and increased laser intensity (45%).

demonstrated that sodium adducts produce the highest abundances and that cation preferences for MC-12, end-capped thread, and rotaxane are all in the order $[M + Na]^+ > [M + Li]^+ \gg [M + Ag]^+$. Spectra obtained using lithium salt also contained sodium adduct peaks irrespective of the amount of lithium salt added. In addition, the ion abundance with any cation was highest with dithranol as the matrix and decreased in the order dithranol ≫ IAA > 2,4-DHB. Thus, we used dithranol matrix and NaTFA salt to prepare all other samples.

To favor desorption and detection of the higher molecular weight molecules/ions observed in the spectrum in Figure 6a, the original sample preparation was analyzed using a higher laser intensity and a longer time interval (corresponding to a higher m/z value) for the low-mass ion deflection in order to deflect the MC-12 and end-capped PTHF thread ions and prevent them from reaching the detector, thus precluding possible detector saturation by the lower-mass ions. The resulting spectrum is expanded in Figure 6b; it contains only peaks above m/z 2000 (full mass range spectrum not shown). There are four molecular weight distributions, with the components present in the highest concentrations separated by 72.1 Da, which is the molecular weight of one THF repeat unit. The four distributions therefore correspond to PTHF with 1−5 repeat units, with the 3-mer present in the highest concentration. The components within each of these four distributions are separated by 44.0 Da, which is the molecular weight of one EO repeat unit, with the 10-mer present in the highest concentration in all four cases. The m/z values match the calculated monoisotopic masses for a series of rotaxanes corresponding to one MC-12 ring of n = 8−14 EO units threaded with one end-capped PTHF thread of m = 1−5 THF units. For example, the peak for a rotaxane complex ion with n = 10 and m = 3 at m/z 2359.7 (the most intense peak in the spectrum) matches the value of 2360.3 Da calculated from the sum of the masses of a sodium cation (23.0 Da), an MC-12 "end group" (290.2 Da), the combined ECT end groups (1390.9 Da), 10 EO units (33 atoms) from MC-12, and three THF units from the end-capped thread.

Potential Fragmentation of MC-12, End-Capped PTHF Thread, and Their Rotaxane. Although we were able to positively identify the rotaxane by MALDI-ToF MS (Figure 6), its signal intensity is significantly lower than that of either MC-12 or the end-capped PTHF thread in the mixture. This may simply be due to a low synthetic yield of rotaxane and/or to the mass spectrum not accurately reflecting the isolated mixture's composition. For example, the rotaxane may ionize less efficiently than the individual MC-12 and end-capped PTHF threads, or it may decompose during the MS analysis. However, if the latter occurs, the rotaxane would have to decompose into the complete macrocycle and complete end-capped thread, rather than either of their fragments, to generate the spectrum shown in Figure 6a. We therefore carried out additional mass spectrometric analyses to investigate the low signal intensity of the rotaxane in MALDI-ToF MS spectra.

Peaks observed using the reflectron analyzer but not the linear analyzer are from post-source decay or metastable fragmentation of the precursor ions during their flight between the ion source and the detector. Since fragment ions have the same velocity but different masses and kinetic energies than the precursor ion, the precursor and fragment ions reach the linear detector at the same time, whereas they are separated in the reflectron mode by mass and time due to their different kinetic energies. Thus, the fragment ions are observed at the same m/z value as the precursor ion in the linear mode, but at different m/z values in reflectron mode. The MALDI mass spectra of the MC-12 and ECT regions, respectively, of the rotaxane sample using both reflectron and linear analysis/detection modes are presented in Figures 7a and 7b. The reflectron and linear mode spectra contain the same major and minor peaks. Thus, we can exclude the possibility of post-source fragmentation of the MC-12 and ECT ions and of the rotaxane ions into MC-12 and/or thread ions, during their time-of-flight, although this comparison cannot rule out in-source decay.

If the rotaxane fragments into MC-12 and/or the end-capped PTHF thread during MALDI-ToF MS analysis, the amount of fragmentation should also depend on the laser power. Figure 8 shows the spectra of the rotaxane sample collected at 25, 30, 35, and 40% of the maximum laser power. The threshold laser power needed to detect the rotaxane ion was 25% of maximum. At 40% of the maximum laser power, new peaks appear that are most likely due to fragmentation. Increasing the laser power increased the abundances of the MC-12 and end-capped thread, with the detector saturated by MC-12 ions at 40% of the maximum laser power. However, their intensity ratio remained fairly constant over large changes in laser power. This indicates that either the rotaxane ion does not fragment significantly or there is

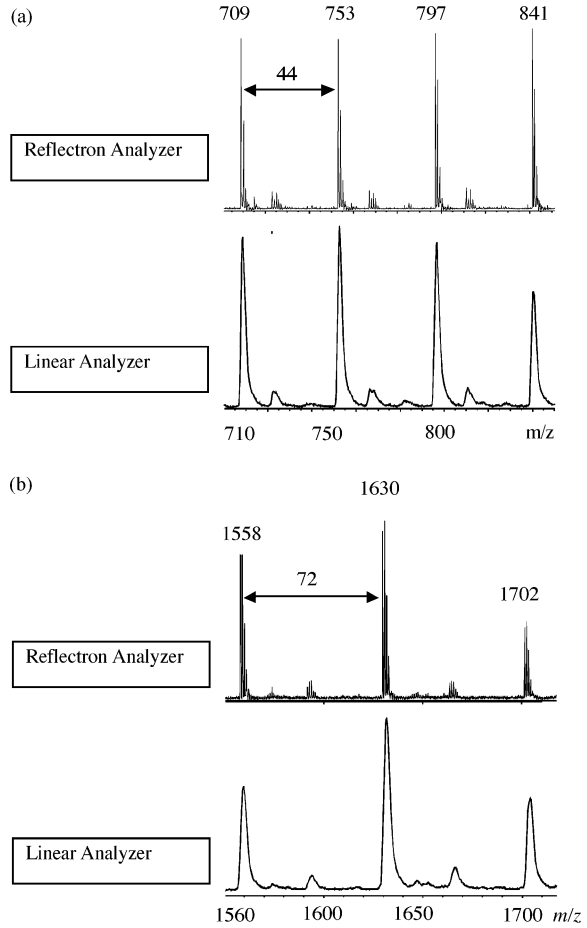

Figure 7. Comparison of the reflectron and linear analysis modes in the partial matrix-assisted laser desorption/ionization time-of-flight mass spectra (dithranol matrix, sodium trifluoroacetate salt) of the "original" rotaxane sample of MC-12 threaded with bis(3-aminopropyl)-terminated poly(tetrahydrofuran)-350 (PTHF) showing the *m/z* regions of (a) MC-12 and (b) end-capped PTHF thread.

no preferential formation of either component from its fragmentation.

Increasing the laser power also increased the abundances of the MC-12 and ECT ions relative to that of the rotaxane ions. This indicates that the rotaxane ionizes less efficiently than either MC-12 or the end-capped PTHF thread and that the cation coordination sites in the rotaxane are therefore less readily accessible than in the nonthreaded components. In addition, varying the laser power does not enhance ionization of either MC-12 or the end-capped thread relative to each other in a mixture of the two. Figure 9 plots the MALDI-ToF MS intensities of the MC-12 11-mer signal at *m/z* 797, and the ECT 3-mer signal at *m/z* 1630, from a 1:1 molar mixture of pure MC-12 and pure end-capped PTHF thread as a function of laser power. Their relative intensities are approximately equal at laser powers of 35−60%. MC-12 and the PTHF end-capped thread therefore have similar ionization efficiencies over a wide range of laser powers.

While the ESI process did not form sufficiently abundant rotaxane ions for tandem MS experiments, ESI-QIT tandem MS (MS^2) experiments were performed on individual MC-12 and ECT oligomers to determine their gas-phase fragmentation patterns. MC-12 readily ionized to form a series of $[MC\text{-}12 + Na]^+$ ions. The MS^2 spectrum of the isolated and fragmented 11-mer (*m/z* 797.5) is shown in Figure 10a. The collisionally activated dissociation of *m/z* 797.5 produced a dominant fragment ion at *m/z* 611.4 by the loss of 186.1 Da. This dissociation corresponds to loss of the hydrocarbon tail of MC-12 as the neutral molecule $HO(CH_2)_{12}H$ (theoretical mass 186.2 Da). The end-capped PTHF thread sample was ionized separately to form a series of $[ECT + Na]^+$ oligomer ions. The MS^2 spectrum (Figure 10b) of the isolated and fragmented 3-mer (*m/z* 1631.2 Da) shows

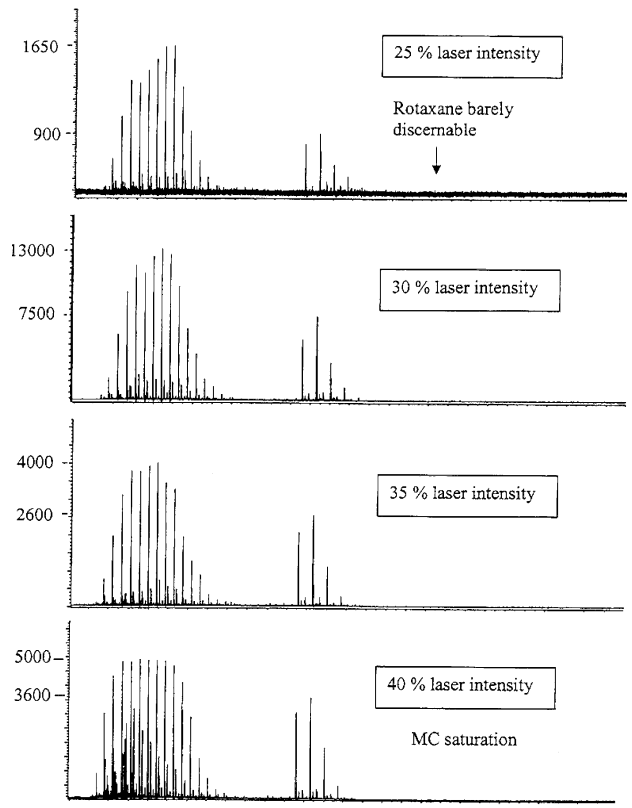

Figure 8. Matrix-assisted laser desorption/ionization time-of-flight mass spectra (dithranol matrix, sodium trifluoroacetate salt, reflectron mode) of the "original" rotaxane sample of MC-12 threaded with bis(3-aminopropyl)-terminated poly(tetrahydrofuran)-350 over a series of laser intensities (25, 30, 35, and 40% of maximum laser power); *y*-axis numbers denote the approximate intensity of the 11-mer of MC-12 (*m/z* 797; top number) and the 3-mer of the end-capped PTHF thread (*m/z* 1690; bottom number).

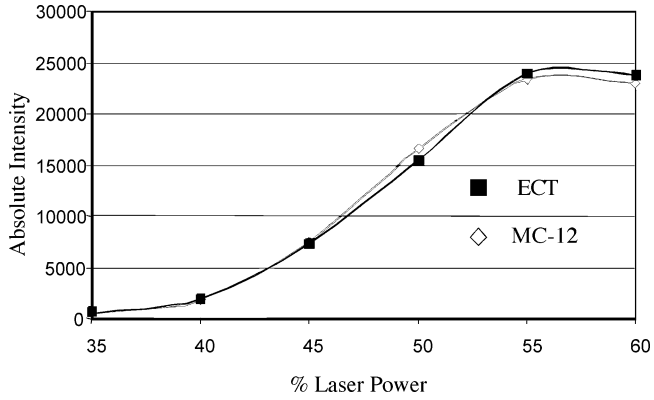

Figure 9. Comparison of matrix-assisted laser desorption/ionization time-of-flight mass spectra signal intensities for a 1:1 molar mixture of pure MC-12 (11-mer at *m/z* 797) and pure end-capped PTHF thread (ECT; 3-mer at *m/z* 1630) in dithranol in the presence of sodium trifluoroacetate as a function of laser power (percentage of the maximum power available); MC-12 and ECT each at 10^{-5} M in THF; 5:1:1 matrix/salt/polymer.

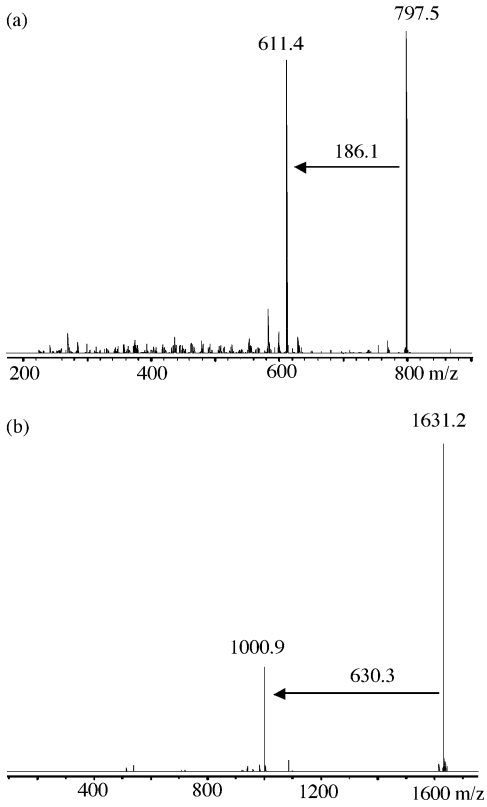

Figure 10. Electrospray ionization quadrupole ion trap MS/MS spectra of (a) MC-12 (11-mer at *m/z* 797.5) and (b) end-capped PTHF thread (3-mer at *m/z* 1631.5) in the presence of sodium trifluoroacetate.

a dominant fragment ion at *m/z* 1000.9, arising from the loss of 630.3 Da from the precursor ion. This corresponds to loss of the azlactone end-capping group through cleavage of the amide bond by intramolecular ring closure, as outlined in Scheme 5; in analogy to the mechanism established for dissociation of protonated peptides,[17] Na^+ remains coordinated with the amine fragment. However, these fragment ions are not observed in the MALDI-ToF MS spectra of the rotaxane mixture, which contains only intact thread and macrocycle ions. This indicates that the rotaxane is not fragmenting in the MS analysis, although it may not follow the same fragmentation mechanisms as the individual components.

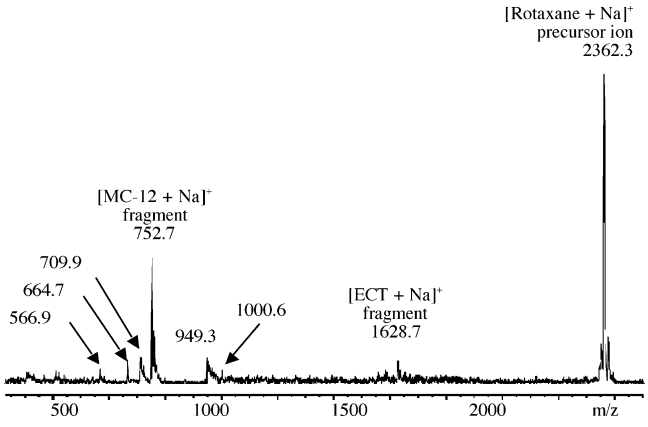

Figure 11. Composite post-source decay time-of-flight MS/MS spectrum of the rotaxane $[M + Na]^+$ ion composed of the 10-mer of MC-12 of mass 730 Da, the 3-mer of the end-capped PTHF thread (1607 Da), and a sodium cation of mass 23.0 Da.

The rotaxane ion was analyzed by post-source decay (PSD) tandem MS to investigate its actual fragmentation pathways upon MALDI; the mass accuracy of PSD spectra is poor, with observed *m/z* values often being up to 2 units off from calculated mass-to-charge ratios. The resulting PSD spectrum is shown in Figure 11. The $n = 10$ EO (730 Da)/$m = 3$ THF (1607 Da) rotaxane oligomer at *m/z* 2360 was isolated for the MS/MS experiment. The $[\text{rotaxane} + Na]^+$ ion (theoretical mass 2360.6 Da, observed at *m/z* 2362.3) produced fragment ions of the complete macrocycle $[\text{MC-12} + Na]^+$ (theoretical mass 753.5 Da, observed at *m/z* 752.7) and the complete end-capped thread $[\text{ECT} + Na]^+$ (theoretical 1630.1 Da, observed *m/z* 1628.7). A few of the other peaks, such as the skewed *m/z* 709.9 and 949.3 peaks, may be artifacts resulting from combination of the various spectral segments. Although the intensities of the peaks cannot be quantitatively compared due to different voltage parameters and laser intensities used for the different spectral regions, the signal-to-noise ratio of the MC-12 fragment ion is qualitatively much greater than that of the ECT fragment ion, implying that more MC-12 ions are created during this intentional fragmentation. This strongly suggests that the preferential dissociation pathway of $[\text{rotaxane} + Na]^+$ involves bond cleavage at the end-capped PTHF thread, enabling complete MC-12 ions to dethread. Indeed, the PSD spectrum contains a peak at *m/z* 1000.6 which

Scheme 5. Proposed Fragmentation of the End-Capped Poly(tetrahydrofuran) (PTHF) Thread by Loss of Azlactone (630 Da); B Represents an Internal Basic Site of the $[\text{ECT} + Na]^+$ Ion

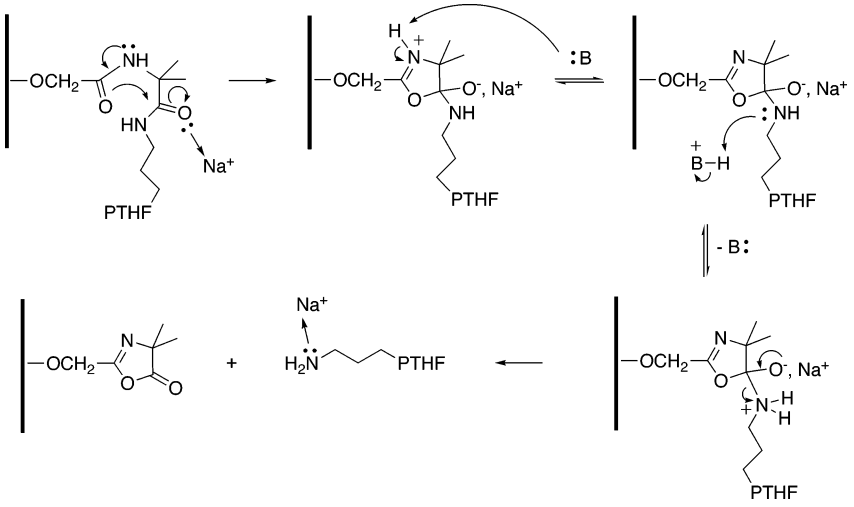

corresponds to the product ion created from the loss of the azlactone end-capping group (630 Da) from the thread, as observed in the ESI MS/MS spectrum of $[ECT + Na]^+$ (Figure 10b). Similarly, the peak at *m/z* 566.9 in the PSD spectrum corresponds to fragmentation of MC-12 by loss of its 186 Da hydrocarbon tail, as was also observed upon ESI MS/MS of $[MC\text{-}12 + Na]^+$ (theoretical mass 567.5 Da) (Figure 10a).

Therefore, the PSD fragmentation pattern of the rotaxane ion shows not only that it may decompose into its individual components but also that if it does fragment, the resulting component ions should also undergo some consecutive fragmentation. Since only the complete MC-12 and end-capped thread ions were present in the original MS spectrum, and the relative abundance of $[ECT + Na]^+$ was substantially higher in the original MS spectrum than upon the deliberate decomposition of $[rotaxane + Na]^+$ in the PSD experiment, the MC-12 and end-capped PTHF thread ions observed in the MS spectrum must be components of the product mixture isolated from the threading experiment and not from any in-source fragmentation of $[rotaxane + Na]^+$ upon MALDI. Such fragmentation behavior also implies that the MC-12 and ECT ions observed in the MS spectrum (where they have comparable relative abundances) cannot be produced by in-source fragmentation either.

MS and HPLC Analysis of Crude and Further-Purified Rotaxane Samples. The low signal intensity of the rotaxane in the MALDI-ToF MS spectra (e.g., Figure 6) is evidently not due to its fragmentation, although there is a contribution from the rotaxane ionizing less efficiently than the nonthreaded components. The more readily ionized MC-12 and end-capped PTHF thread yield ion abundances with a high signal-to-noise ratio, which prevents observation of the less readily ionized rotaxane, whose ion abundance suffers from a lower signal-to-noise ratio. We therefore attempted to purify the rotaxane further by reprecipitation to reduce its contamination with nonthreaded MC-12 and end-capped thread and to better detect the rotaxane ion by MS. Figure 12 compares the MALDI-ToF mass spectra of the crude product (after removing hydrolyzed excess end-capping agent) from the threading experiment and the "further-purified" sample to that of the original rotaxane sample presented thus far (Figure 12b). The spectrum of the crude sample (Figure 12a) is dominated by MC-12 ions, which was used in excess in the threading procedure. The spectrum of the "further-purified" sample (Figure 12c) shows less MC-12 and rotaxane ions compared to the ECT ions. This variation in the relative ion intensities after chromatography and reprecipitation separations confirms that the MALDI process did not fragment the rotaxane into MC-12 and the end-capped PTHF thread. It also again demonstrates the difficulty of isolating a rotaxane from its cyclic and linear components when they are based on identical or similar chemical structures.

Simultaneously with the MS experiments, we investigated both GPC and HPLC to establish conditions at which the three components of the rotaxane mixture would elute separately in order to quantify their relative amounts. We limited the conditions to varying the polarity of the eluant by adding hexanes, methanol, or an electrolyte to THF, using a porous polystyrene GPC column, a silica analytical column, or a C18-coated silica analytical column; all of the conditions investigated are

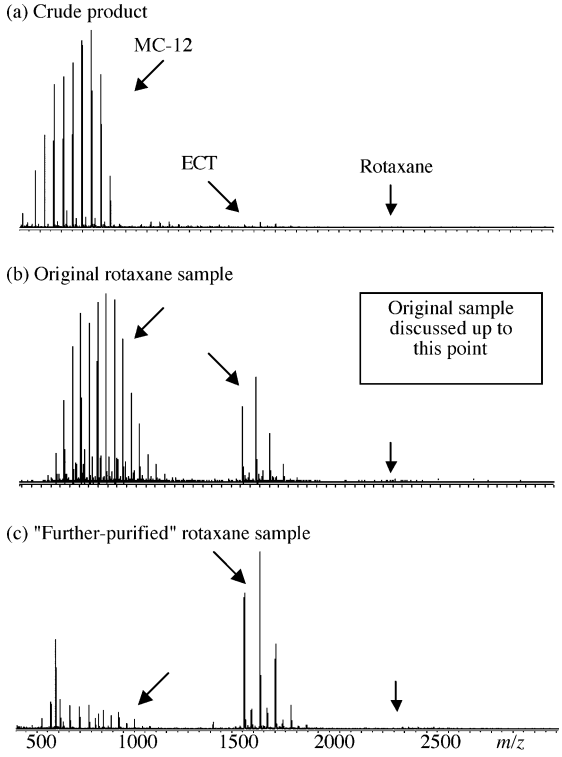

Figure 12. Matrix-assisted laser desorption/ionization time-of-flight mass spectra of rotaxane samples at different stages of purification; dithranol as matrix, NaTFA salt, reflectron mode.

listed in Table S1 of the Supporting Information. Since the three components seemed to separate using the analytical silica column and an eluant of THF containing 0.3 wt % Aliquat 336 $[(H(CH_2)_8)_3NMe^+Cl^-]$, we connected our second silica HPLC column (semipreparative scale) to it to generate the UV-detected chromatogram shown in Figure 13a. MC-12 evidently interacts more strongly with the column than either the end-capped thread or the rotaxane and elutes from the column last. The end-capped thread interacts the least with the column, presumably due to both the fewer number of polar groups and the greater spacing between oxygen atoms in the THF repeat units. The rotaxane elutes at an intermediate position; although it has the greatest number of polar groups, they are less accessible than in the nonthreaded structures, as also indicated by the lower ionization efficiency of the rotaxane by MALDI mass spectrometry.

Figure 13b plots the UV detector response at 254 nm as a function of the concentration of both MC-12 and the end-capped PTHF thread; the end-capped thread, with its eight aromatic rings, absorbs much more strongly than MC-12, with its single aromatic ring. Since we do not have pure rotaxane, nor have an independent method for determining its concentration in a mixture, we were not able to calibrate the UV detector response for the rotaxane concentration. Assuming that the absorbance of the rotaxane corresponds to the sum of the absorbances of MC-12 and the end-capped thread, the "further-purified" rotaxane sample is composed of 66 wt % end-capped PTHF thread, 23 wt % MC-12, and 11 wt % rotaxane, which is similar to the qualitative composition indicated by the MALDI ToF mass spectrum in Figure 12c. The amount of rotaxane in the crude product was evidently too low to be detected by HPLC, which is qualitatively similar to the composi-

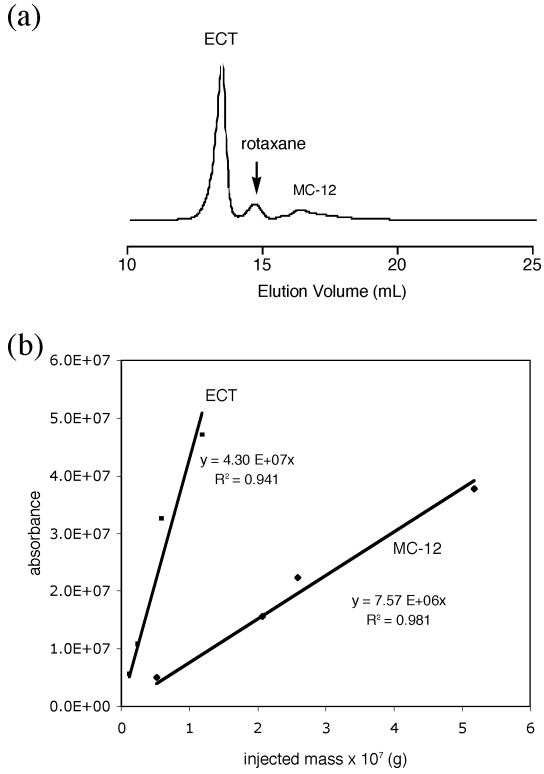

Figure 13. (a) UV-detected high-performance liquid chromatogram of the further-purified rotaxane sample using a semipreparative scale and an analytical silica gel column (10 μm particles, 125 Å pores) connected in series, and 1 mL/min tetrahydrofuran containing 0.3 wt % Aliquat 335 as the eluant at 35 °C. (b) The corresponding calibration plots of the MC-12 and end-capped poly(tetrahydrofuran) thread components.

tion indicated by the MALDI ToF mass spectrum in Figure 12a. The 11 wt % rotaxane in the "further-purified" sample corresponds to an overall yield of 4.8% rotaxane in this particular fraction, which underestimates the exact value due to the presence of rotaxane, MC-12, and end-capped thread in almost all fractions obtained. Nevertheless, this low yield of rotaxane is consistent with our simulation results, in which we found that planar alignment (as in a lamellar mesophase) of the macrocycles will result in no more than 10% of the rings threaded in an equimolar mixture of 42-crown-14 and $CH_3(OCH_2CH_2)_{13}OCH_3$,[8] which is twice the amount of statistical threading in the melt.

Conclusions

Pure amphiphilic macrocrown ether (MC-12) was obtained by separating out linear and higher order cyclic oligomers following the macrocyclization synthetic step by a combination of column chromatography and Soxhlet extraction. According to MALDI-ToF MS, the ring produced in the highest concentration in repetitions of the synthesis of MC-12 varies from 9 to 12 EO repeat units. Pure MC-12 was used to synthesize a rotaxane composed of one MC-12 ring threaded with one end-capped PTHF thread, which is very difficult to separate and isolate from its two components. The rotaxane was conclusively detected by MS, with the average rotaxane consisting of an MC-12 ring with 11 EO repeat units and a thread with three THF repeat units. The signal intensity of this rotaxane was significantly lower than those of the nonthreaded MC-12 and end-capped PTHF thread contaminating the sample. This low signal intensity was due to the low synthetic yield (<10%) of the rotaxane and to its low ionization efficiency compared to that of MC-12 and the end-capped PTHF thread. Both the low MALDI-ToF MS ionization efficiency of the rotaxane and its intermediate HPLC elution behavior (relative to its two components) demonstrate that the heteroatoms in the rotaxane are less accessible to coordinating species than those of its components. ESI-QIT MS/MS experiments and a comparison of ToF reflectron and linear mode spectra demonstrated that the rotaxane does not fragment during its time-of-flight. A post-source decay MS/MS analysis demonstrated that it also does not undergo in-source fragmentation.

HPLC of the rotaxane demonstrated that it elutes separately from both the end-capped thread and MC-12 using silica columns and an eluant of 0.3 wt % $[H(CH_2)_8]_3NMe^+Cl^-$ in THF at 35 °C. The composition of a "further-purified" sample of the rotaxane confirmed that its MALDI-ToF mass spectrum was qualitatively correct and that it consisted of 66 wt % end-capped PTHF thread, 23 wt % MC-12, and 11 wt % rotaxane. The use of solutions of MC-12 organized into lamellar mesophases will therefore not generate threaded structures in sufficient quantity to enable extensive characterization of their properties, especially considering how difficult it is to separate the rotaxane from its two components. However, we anticipate that threading will be better promoted in solutions of the macrocycle organized into a columnar mesophase and will therefore explore this possibility in the future.

Acknowledgment is made to NASA Glenn Research Center and the Ohio Board of Regents for financial support of this research. Generous support for the acquisition of the mass spectrometers used in this study was provided by the National Science Foundation and the Ohio Board of Regents (Hayes Investment Fund).

Supporting Information Available: Conditions for optimizing GPC and/or HPLC conditions for separating and quantifying the composition of mixtures of MC-12, end-capped PTHF thread, and their rotaxane. This material is available free of charge via the Internet at http://pubs.acs.org.

References and Notes

(1) (a) Schill, G. *Catenanes, Rotaxanes and Knots*; Academic Press: New York, 1971. (b) Preece, J. A.; Stoddart, J. F. *Nanobiology* **1994**, *3*, 149−166. (c) Amabilino, D. B.; Stoddart, J. F. *Chem. Rev.* **1995**, *95*, 2725−2829. (d) Amabilino, D. B.; Raymo, F. M.; Stoddart, J. F. In *Comprehensive Supramolecular Chemistry*; Lehn, J.-M., Ed.; Pergamon Press: Oxford, 1996; Vol. 9, Chapter 3. (e) Vogtle, F.; Dunnwald, T.; Schmidt, T. *Acc. Chem. Res.* **1996**, *29*, 451−460. (f) Chambron, J. C. *Persp. Supramol. Chem.* **1999**, *5*, 225−284. (g) Breault, G. A.; Hunter, C. A.; Mayers, P. C. *Tetrahedron* **1999**, *55*, 5265−5293. (h) Panova, I. G.; Topchieva, I. N. *Russ. Chem. Rev.* **2001**, *70*, 23−44.

(2) (a) Gibson, H. W.; Bheda, M. C.; Engen, P. T. *Prog. Polym. Sci.* **1994**, *19*, 843−945. (b) Sauvage, J. P., Dietrich-Buchecker, C., Eds.; *Molecular Catenanes, Rotaxanes and Knots*; Wiley-VCH Verlag GmbH: Weinheim, Germany, 1999.

(3) (a) Gibson, H. W.; Marand, H. *Adv. Mater.* **1993**, *5*, 11−21. (b) Ogino, H. *New J. Chem.* **1993**, *17*, 683. (c) Amabilino, D. B.; Parsons, I. W.; Stoddart, J. F. *Trends Polym. Sci.* **1994**, *2*, 146−152. (d) Raymo, F. M.; Stoddart, J. F. *Trends Polym. Sci.* **1996**, *4*, 208−211. (e) Harada, A. *Coord. Chem. Rev.* **1996**, *148*, 115−133. (f) Gong, C.; Gibson, H. W. *Curr. Opin. Solid State Mater. Sci.* **1997**, *2*, 647−652. (g) Harada, A. *Acta Polym.* **1998**, *49*, 3−17. (h) Harada, A. *Mater. Sci. Tech.* **1999**, *20*, 485−512. (i) Raymo, F. M.; Stoddart, J. F. In *Supramolecular Polymers*; Diferri, A., Ed.; Marcel Dekker: New York, 2002; pp 323−357. (j) Cardin, D. J. *Adv. Mater.* **2002**, *14*, 553−563.

(4) Pugh, C.; Bae, J.-Y.; Scott, J. R.; Wilkins, C. L. *Macromolecules* **1997**, *30*, 8139−8152.
(5) Brandys, F. A.; Pugh, C. *Macromolecules* **1997**, *30*, 8153−8160.
(6) Xu, G.; Rane, S. S.; Helfer, C. A.; Mattice, W. L.; Pugh, C. *Modeling Simul. Mater. Sci. Eng.* **2004**, *12*, S59−S71.
(7) Rane, S. S.; Mattice, W. L.; Pugh, C. *J. Chem. Phys.* **2004**, *120*, 10299−10306.
(8) Helfer, C. A.; Xu, G.; Mattice, W. L.; Pugh, C. *Macromolecules* **2003**, *36*, 10071−10078.
(9) MC-12 is a hydrophilic macrocrown ether with an average ring size of 42 atoms, functionalized with a hydrophobic 12-carbon tail.
(10) (a) Crossland, R. K.; Servis, K. L. *J. Org. Chem.* **1970**, *35*, 3195−3196. (b) Harrison, I. T. *J. Chem. Soc., Perkin Trans. 1* **1974**, *2*, 301−304.
(11) See for example: (a) Rasmussen, J. K.; Heilmann, S. M.; Krepski, L. R. In *Encyclopedia of Polymer Science and Engineering*, 2nd ed.; Mark, H. F., Bikales, N., Overberger, C. G., Menges, G., Eds.; Wiley-Interscience: New York, 1988; Vol. 11, pp 558−571 and references therein. (b) Taylor, L. D.; Kolesinski, H. S.; Mehta, A. C.; Locatell, L.; Larson, P. S. *Makromol. Chem., Rapid Commun.* **1982**, *3*, 779−781. (c) Heilmann, S. M.; Rasmussen, J. K.; Palensky, F. J.; Smith, H. K., II *J. Polym. Sci., Polym. Chem. Ed.* **1984**, *22*, 1179−1186.
(12) Drtina, G. J.; Heilmann, S. M.; Moren, D. M.; Rasmussen, J. K.; Krepski, L. R.; Smith, H. K., II; Pranis, R. A.; Turek, T. C. *Macromolecules* **1996**, *29*, 4486-4489 and references therein.
(13) Although we previously reported that MC-12, which was contaminated with ∼17% of its cyclic dimer, did not dissolve completely in hexanes,[4,5] we have found that pure MC-12 is soluble in hexanes.
(14) *User's Guide to the Reflex III MALDI-TOF Mass Spectrometer*; Bruker Analytical Systems, Inc.: Billerica, 1999.
(15) Nielen, M. W. F. *Mass Spectrom. Rev.* **1999**, *18*, 309−344.
(16) (a) Von Helden, G.; Wyttenbach, T.; Bowers, M. T. *Science* **1995**, *267*, 1483−1485. (b) Reinhold: M.; Meier, R. J.; de Koster, C. G. *Rapid Commun. Mass Spectrom.* **1998**, *12*, 1962−1966.
(17) (a) Paizs, B.; Suhai, S. *J. Am. Soc. Mass Spectrom.* **2004**, *15*, 103−113. (b) Wang, P.; Kish, M. M.; Wesdemiotis, C. *The Encyclopedia of Mass Spectrometry*; Gross, M. L., Caprioli, R., Eds.; Elsevier: Amsterdam, 2005; Vol. 2, Part A, pp 139−151.

MA0476689